SUBBAND ENCODING BY WAVELET FILTER CASCADE FOR BANDWIDTH COMPRESSION IN FDTD SIMULATION*

M.G. Mayes[ξ], C.D. Cantrell[Ψ]
Applied Physical Electronics L.C. PO Box 341149
Austin,TX,USA

Abstract

The wavelet filter cascade method for subband encoding of finite-difference time-domain simulation is presented. This method implements computational bandwidth compression via a filter bank comprised of discrete wavelet transforms which maps simulation data or measured data into a compressed representation with little degradation of signal integrity. This letter discusses the use of the WFC technique to augment the FDTD method in particular but may be extended to other time domain methods. Simulation results are compared to standard FDTD results for accuracy and signal fidelity, with reduction in problem size summarized.

I. INTRODUCTION

Due to the transient nature of electromagnetic pulse discharge, frequency domain techniques, which bypass the transient phase by mapping directly to the steady state, do not accurately characterize pulse dynamics. Time domain methods as the FDTD are employed to advance simulation through time transients and the spatial near-field [1]. However, abrupt pulse transitions generate high frequencies and considerable computational bandwidth which render large scale time-domain simulations intractable for most desktop machines.

A broad range of temporal frequencies indicates use of a multi-resolution time-domain method in order to adapt time increment to frequency components [3]. Existing MRTD techniques introduce multiple spatial granularities to a uniformly meshed domain for enhanced economy of computation in a problem space with wide variation in spatial scales [2] [4] [5]. The MRTD method first expands the spatial aspect of the electromagnetic field with a wavelet orthogonal expansion followed by the Galerkin discretization procedure to generate the system matrix that describes the field within the computational domain. The time aspect of the field is represented by a pulse basis. Due to exponential decay of inner product terms between expansion functions, higher order terms may be neglected so that system matrix entries are concentrated on sub-diagonals, diagonal, and super-diagonals. This enables use of sparse matrix methods for substantial savings in computational operations [2].

The technique presented in this letter differs from the MRTD method by use of the discrete wavelet transform in a filter bank that transforms a pulse time series into a reduced representation. The filter bank arrangement of the DWT is termed the wavelet filter cascade and builds upon the formalism and design rules in [3].

The WFC implements wavelet decomposition in the time domain that partitions the field into frequency subbands. Subband encoding is the frequency domain equivalent of multiresolution in signal space. The partition of pulse bandwidth yields a reduction in sampling frequency for each subband, which corresponds to a lengthened time step and thus space step. Field components then propagate within the sub-domains with a reduced number of computations. This method avoids use of the high sampling rate required by the total field.

II. THEORY

The wavelet filter cascade method is based upon the concept of the quadrature mirror filter. The analysis branch of the QMF performs coding, i.e. transformation of signal format, while the synthesis branch decodes filter products to restore the signal to its original format [3]. A filter bank is constructed by a lattice of the basic QMF unit cell. The wavelet QMF is constructed with discrete wavelet transforms as filters.

A. Subband Encoding

Subband encoding is the process whereby an analysis filter bank decomposes a signal into separate frequency bands, implementing multirate signal processing. This is an effective method for compressing signal representation, so that when combined with adaptive bit allocation among filter products, it achieves reduction in sampling rate for the total signal [3].

B. Quadrature Mirror Filter

The QMF is a filter cascade comprised of M complementary filters that separate a signal into M frequency subbands. This action reduces sampling frequency of subbands by a factor of M [3]. Figures 1 and 2 illustrate branches of a simple two-channel QMF. The analysis branch consists of tandem lowpass ($\underline{L}$) and highpass ($\underline{H}$) filters with mirror symmetry about $\pi/2$ while the synthesis branch has a symmetrically opposite

* Work supported in part by the US Missile Defense Agency under contract number DASG60-02-P-0090.
ξ email: mgmayes@apelc.com
Ψ PhoTEC, Department of Electrical Engineering, University of Texas at Dallas, MS EC33, PO Box 830688, Richardson Texas, 75083-0688. Email: Cantrell@utdallas.edu.

arrangement. To eliminate redundant information, the output arrays are downsampled, or decimated, by a factor of 2, eliminating every other element of the signal series. Decimation in signal space is equivalent to reduction of bandwidth in the frequency domain. For an input signal of length *n*, down-2 yields an *n*/2 length array.

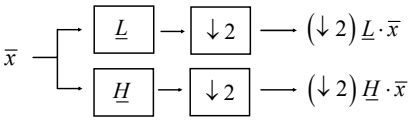

Figure 1. 2-channel QMF analysis branch with down-2 operation

Input signal $\overline{x}$ is recovered by the synthesis branch, which is formed by the inverse filters L^* and H^*.

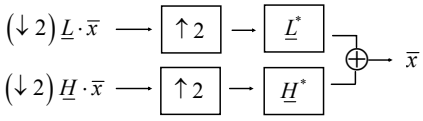

Figure 2. QMF synthesis branch

Filter products $(\downarrow 2)\underline{L}\cdot\overline{x}$ and $(\downarrow 2)\underline{H}\cdot\overline{x}$ are up-sampled with the insertion of zeros between array elements, and interleaved to recover the original signal. In practice, the separate filters in the analysis branch are rows in a DWT matrix; synthesis applies the inverse DWT.

C. The Haar wavelet

The Haar wavelet system is used herein for the description of the WFC encoding method. The Haar DWT is formed by a moving average and a moving difference filter. The Haar transform is given by

$$DWT_H := \frac{1}{\sqrt{2}}\begin{bmatrix}1 & 1\\ 1 & -1\end{bmatrix} \tag{1}$$

with lowpass filter $\underline{L} := [1 \quad 1]/\sqrt{2}$ and highpass filter $\underline{H} := [1 \quad -1]/\sqrt{2}$. Magnitude responses are shown in fig 3 below.

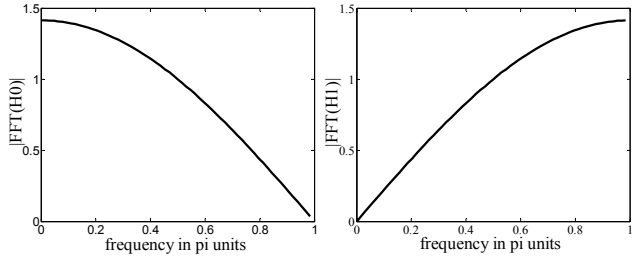

Figure 3. $|FFT(\underline{L})|$ (left), $|FFT(\underline{H})|$ (right)

For the Haar transform (1), inversion in fig 2 is obtained by application of DWT_H^T, where superscript *T* indicates matrix transposition.

D. The wavelet filter cascade

A filter bank is a lattice of filters. The analysis branch encodes the input signal into subband signals with a cascade of filters. We define the wavelet filter cascade as a QMF lattice of discrete wavelet transforms. The basic WFC is the single stage QMF in fig 1 and fig 2. A two-stage WFC may be constructed by repetition of the analysis branch in fig 1 to the lowpass output of the first stage. This is illustrated in figure 4.

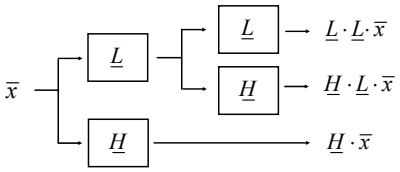

Figure 4. Two stage WFC analysis branch

The corresponding synthesis branch mirrors this construction. We note that the downsampling operation is implicit in fig 2 and following figures.

Filter product $\underline{H}\cdot\overline{x}$ has resolution 2 Δt where Δt is the sample spacing of the original signal. $\underline{H}\cdot\overline{x}$ occupies the highest frequency band of the decomposition products. $\underline{H}\cdot\underline{L}\cdot\overline{x}$ has resolution $4\Delta t$ and occupies the middle band between the three decomposition products. $\underline{L}\cdot\underline{L}\cdot\overline{x}$ has resolution $4\Delta t$ and represents the signal average over the signal duration. Extending fig 2 to a three-level analysis branch, decomposition products are

$$\left\{\underline{H}\cdot\overline{x} \quad \underline{H}\cdot\underline{L}\cdot\overline{x} \quad \underline{H}\cdot\underline{L}^2\cdot\overline{x} \quad \underline{L}^3\cdot\overline{x}\right\}$$

with resolutions $(2\Delta t \quad 4\Delta t \quad 8\Delta t \quad 8\Delta t)$.

E. The augmented FDTD

The FDTD process is inserted between analysis and synthesis branches in figures 1 and 2. The excitation field is transformed to the wavelet representation and propagated with the original algorithm. FDTD time and space steps are first dimensioned for accurate sampling and stable iteration. Once determined, time and space steps are matched by taking equality in the Courant condition

$$\Delta t = \frac{1}{c}\left(\frac{1}{\Delta x^2}+\frac{1}{\Delta y^2}+\frac{1}{\Delta z^2}\right)^{-\frac{1}{2}} \tag{2}$$

[1]. This is the magic time step, and minimizes numerical dispersion. For a uniform mesh, the magic time step is $\Delta t = \Delta/c\sqrt{3}$. Applying a single Haar transform to adjacent samples of a time series results in a pulse train of averages and another of differences, with Δt'=2Δt sample spacing. The corresponding space increment is 2Δ, with $\Delta t' = 2\Delta/c\sqrt{3}$, in accord with (2). The transformed pulse train propagates on a mesh defined by increments (2Δ, 2Δt). The FDTD process on this mesh inherits stability and accuracy from the original mesh.

III. PULSE DECOMPOSITION

In this section, we perform a wavelet decomposition upon a hypothetical pulse to demonstrate the magnitude and distribution of energy filter products.

A. Single stage WFC decomposition

A pulse with both rapid and slow transitions is composed to demonstrate the utility of wavelet decomposition.

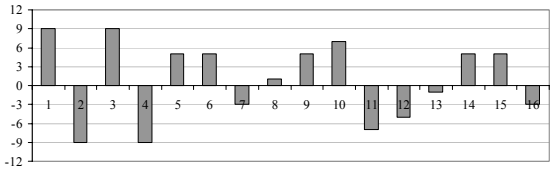

Figure 5. time series $\bar{x}$.

The leading terms in the time series vary abruptly and give rise to high frequency content as seen in fig 6. Abrupt signal transitions yield large moving differences, i.e. highpass filter products. The smoother signal transitions in the later half of the series yield lower frequencies and heavier signal averages.

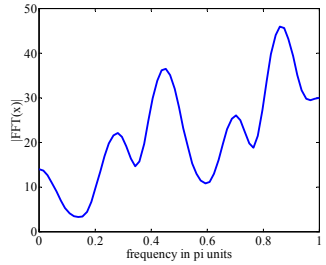

Figure 6. $|FFT(\bar{x})|$, signal in fig 5

The Haar DWT is applied to the time series and gives two half-length time series with spacing 2Δt. With the initial sampling frequency of $f_s = 1/\Delta t$, the sampling frequency is halved.

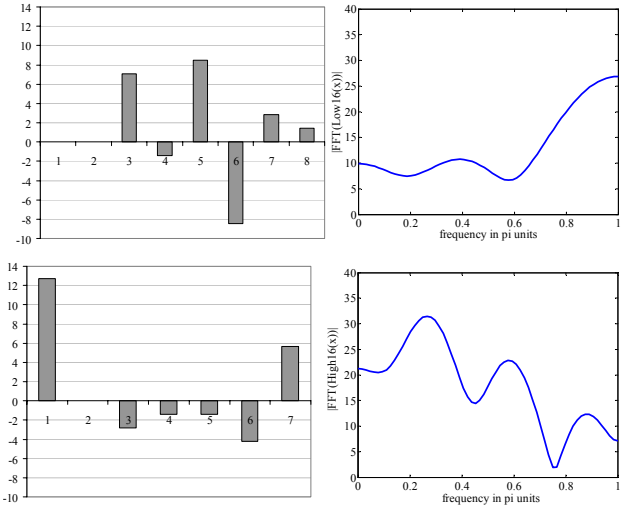

Figure 7. Filter products. Haar lowpass filter product $\underline{L}\cdot\bar{x}$ and $|FFT(\underline{L}\cdot\bar{x})|$ (upper), Haar highpass filter product $\underline{H}\cdot\bar{x}$ and $|FFT(\underline{H}\cdot\bar{x})|$ (lower)

B. Multiple stage WFC decomposition

As illustrated in fig 4, repeated application of the analysis branch of fig 1 leads to further decomposition products. Two and three-level WFC constructions are pictured in the figure below.

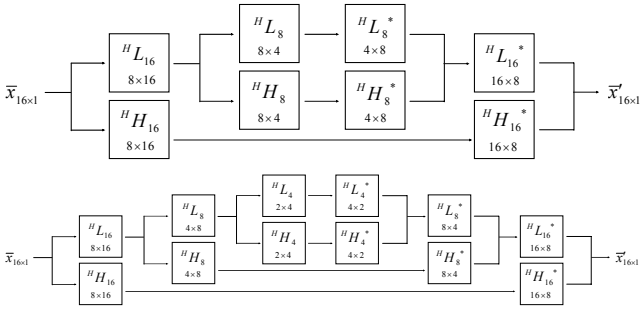

Figure 8. WFC analysis and synthesis branches. Two level, WFC3 (upper), three level WFC4 (lower)

Signal $\bar{x}$ in fig 5 is further decomposed via the two and three stage WFC analysis branches in fig 8. The two-stage, WFC3 in fig 8, yields filter products and resolutions $(\underline{H}\cdot\bar{x}, 2\Delta t)$, $(\underline{H}\underline{L}\cdot\bar{x}, 4\Delta t)$ and $(\underline{L}\underline{L}\cdot\bar{x}, 4\Delta t)$. Three-level WFC4, has filter products $(\underline{H}\cdot\bar{x}, 2\Delta t)$, $(\underline{H}\underline{L}\cdot\bar{x}, 4\Delta t)$, $(\underline{H}\underline{L}\underline{L}\cdot\bar{x}, 8\Delta t)$, and $(\underline{L}\underline{L}\underline{L}\cdot\bar{x}, 8\Delta t)$ Figure 9 details the partition of signal energy among the filter products for each of the WFC decompositions.

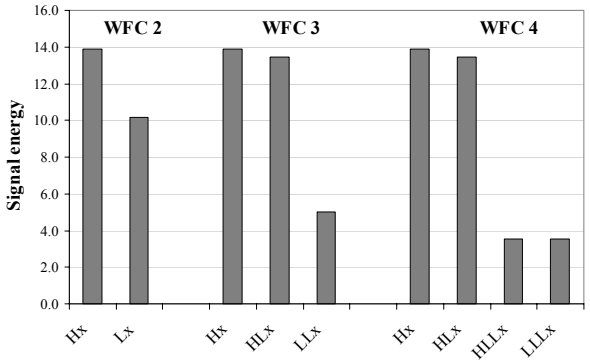

Figure 9. Filter product energies

C. Inversion error

While bandwidth is reduced with continued encoding of filter products, table 1 exhibits the growth in inversion error.

WFC level	RMS error	RMS error (dB)	Relative error
2	8.63E-15	-140.60	1
3	1.27E-14	-139.00	1.47
4	1.31E-14	-138.80	1.52

Table 1. WFC Inversion error: levels 2, 3 and 4

Repeated WFC stages result in loss of total signal energy, typically 1-5%, as detailed in figure 10.

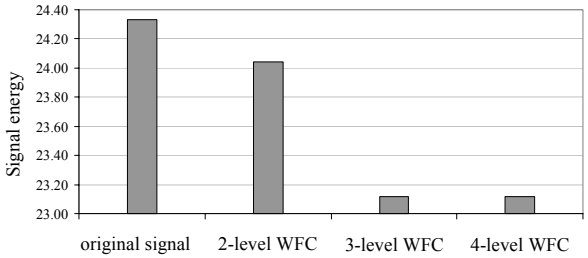

Figure 10. Total energy, original signal and coded-decoded signal for 2, 3 and 4 level WFC

IV. SIMULATION

A. Problem space

The problem space for demonstrating the FDTD+WFC method is a rectangular microwave waveguide comprised of a perfect electrical conductor with vacuum interior. The waveguide cutoff frequency is 3.75 GHz. Simulation was conducted with control and experimental simulations. The control was initialized with spatial increment $\Delta = \lambda/30$, and used the standard FDTD algorithm. The experimental simulation was initialized with spatial increment λ/15, transformed via the Haar DWT, and propagated on the (2Δ,2Δt) mesh. Both simulations were sourced by a two-sample series {1, -0.8} modulating a 5 GHz carrier for a TE_{10} mode. After propagating distances of z = 250λ, 500λ, and 700λ, the power for the first pulse is calculated. In the experimental simulation, the field is propagated over the same distances as the control, whence the transformed pulses are decoded and power calculated for the first pulse.

V. RESUTS AND DISCUSSION

Fig 11 details the difference between the control and experimental simulations. Discrepancies in power fall in the 2.3 to 4.6% range.

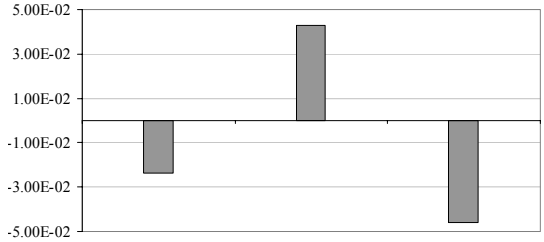

Figure 11. Relative error for propagation distances $z = 250\lambda,\ 500\lambda,\ 700\lambda$.

As discussed in the inversion error section and summarized in fig 10, the Haar DWT introduces a 1 to 3% error floor to computations. Error in fig 11 is explained in part by energy loss in the WFC coding and decoding process. More advanced wavelet systems, e.g. Daubechies [3] and Battle-LeMarie [2] exist that provide lower energy losses in the coding-decoding process. Efforts continue to implement the WFC with greater precision with alternative wavelet systems.

	FDTD+WFC	FDTD
spatial resolution	lambda /15	lambda /30
cells	10 x 15 x Z/2	20 x 30 x Z

Table 2. Control vs. experimental problem space

Table 2 summarizes the total cells for the control and experimental simulations. Because the space increment in the FDTD+WFC simulation is twice that of the control, it requires half the number of cells in each dimension, so the size of each sub-simulation is 1/2·1/2·1/2=1/8 of the original simulation. With two sub-simulations, the total size of the WFC+FDTD problem space is 25% of the original.

VI. SUMMARY

We have described the wavelet filter cascade method for subband coding of FDTD simulations. This method is developed for parsing large time-domain simulations into smaller sub-simulations for serial processing on desk top computers and parallel processing in distributed systems.

REFERENCES

[1] Allen Taflove, Computational Electrodynamics: The Finite-Difference Time-Domain Method. Boston MA: Artech House, 1995.

[2] L.P.B. Katehi, J.F. Harvey, and E. Tentzeris, "Time-Domain Analysis Using Multiresolution Expansions", in Advances in Computational Electrodynamics: The Finite-Difference Time-Domain Method, Allen Taflove, Ed. Boston MA: Artech House, 1998, pp 111-162.

[3] Gilbert Strang and Truong Nguyen, Wavelets and Filter Banks. Wellesley MA, 1997.

[4] Michael Krumpholz and Linda P.B. Katehi, "MRTD: NewTime-Domain Schemes Based on Multiresolution Analysis." IEEE Transactions on Microwave Theory and Techniques, Vol. 44, No. 4, April 1996.

[5] E.M. Tentzeris, A. Cangellaris, L.P.B. Katehi, and J.F. Harvey, "Multiresolution Time-Domain (MRTD) Adaptive Schemes Using Arbitrary Resolutions of Wavelets." IEEE Transactions on Microwave Theory and Techniques, Vol. 50, No. 2, February 2002.

[6] Daniel Zwillinger, Handbook of Differential Equations. Boston MA: Academic Press, 1989.

[7] Stephen Welstead, Fractal and Wavelet Image Compression Techniques. Wellingham WA: SPIE Optical Engineering Press, 1999.

[8] Constantine A. Balanis, Advanced Engineering Electromagnetics. New York: John Wiley & Sons, 1989.